Supporting Information

Bacterial Cellulose-Derived Micro/mesoporous Carbon Anode Materials Controlled by Poly (methyl methacrylate) for Fast Sodium Ion Transport

Fujuan Wang [a], Xiaohong Shi [a], Junlei Zhang [b,c], Tianqi He [b,c], Liang Yang [a], Tianyun Zhang [a,b,*], Fen Ran [b,c,*]

[a] *School of Mechanical and Electronical Engineering, Lanzhou University of Technology, Lanzhou 730050, China*

[b] *State Key Laboratory of Advanced Processing and Recycling of Non-ferrous Metals, Lanzhou University of Technology, Lanzhou 730050, China*

[c] *School of Materials Science and Engineering, Lanzhou University of Technology, Lanzhou 730050, China*

* *Corresponding authors: Dr. Tianyun Zhang (E-mail: zhangtianyunt@163.com or zhangtianyun@lut.edu.cn); and Prof. Fen Ran (E-mail: ranfen@163.com or ranfen@lut.edu.cn)*

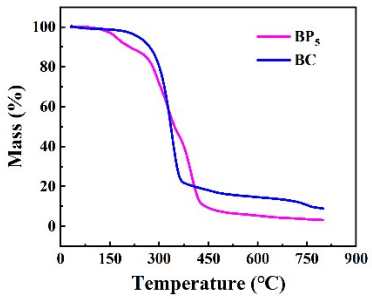

Figure S1 *TGA curves of the BP_5 and pure BC.*

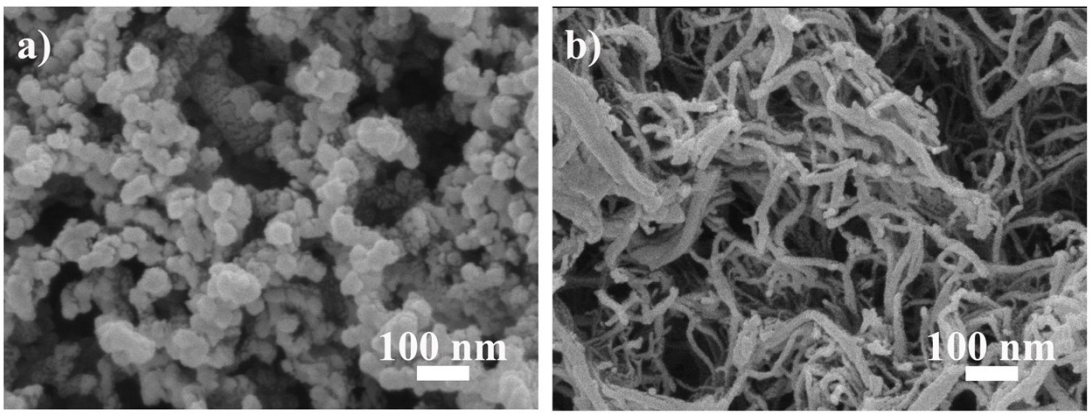

Figure S2 *SEM images for a) c-BC-1050 and b) c-BP_5-1050.*

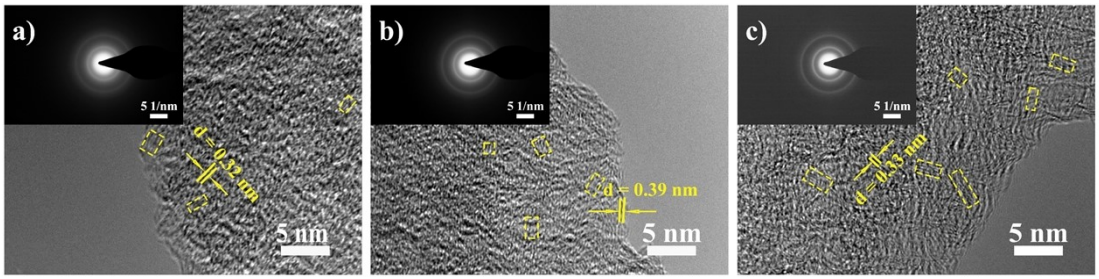

Figure S3 *TEM images for a) c-BP_5-850, b) c-BP_5-1050, and c) c-BP_5-1250.*

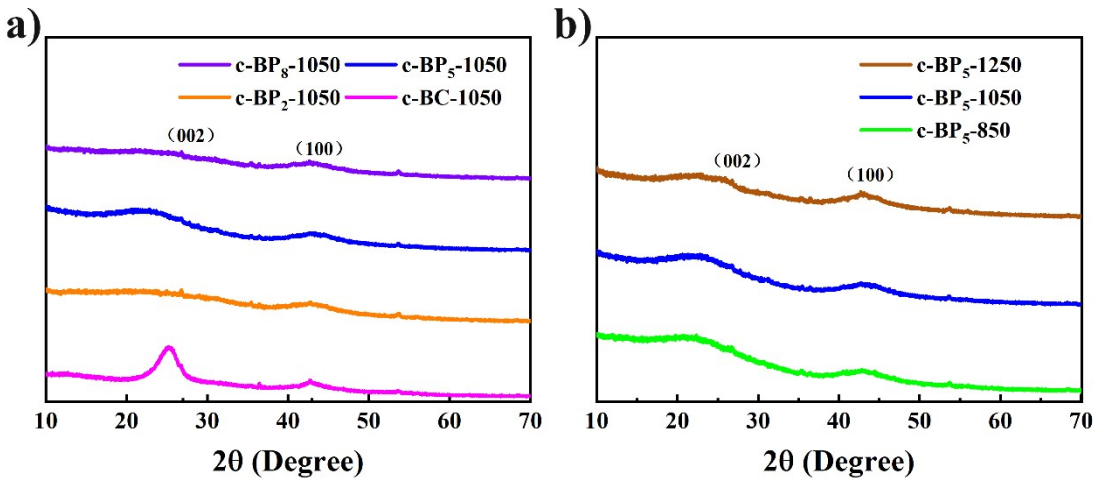

Figure S4 *a) XRD patterns for c-BC-1050, c-BP_2-1050, c-BP_5-1050, and c-BP_8-1050; b) XRD patterns for c-BP_5-850, c-BP_5-1050, and c-BP_5-1250.*

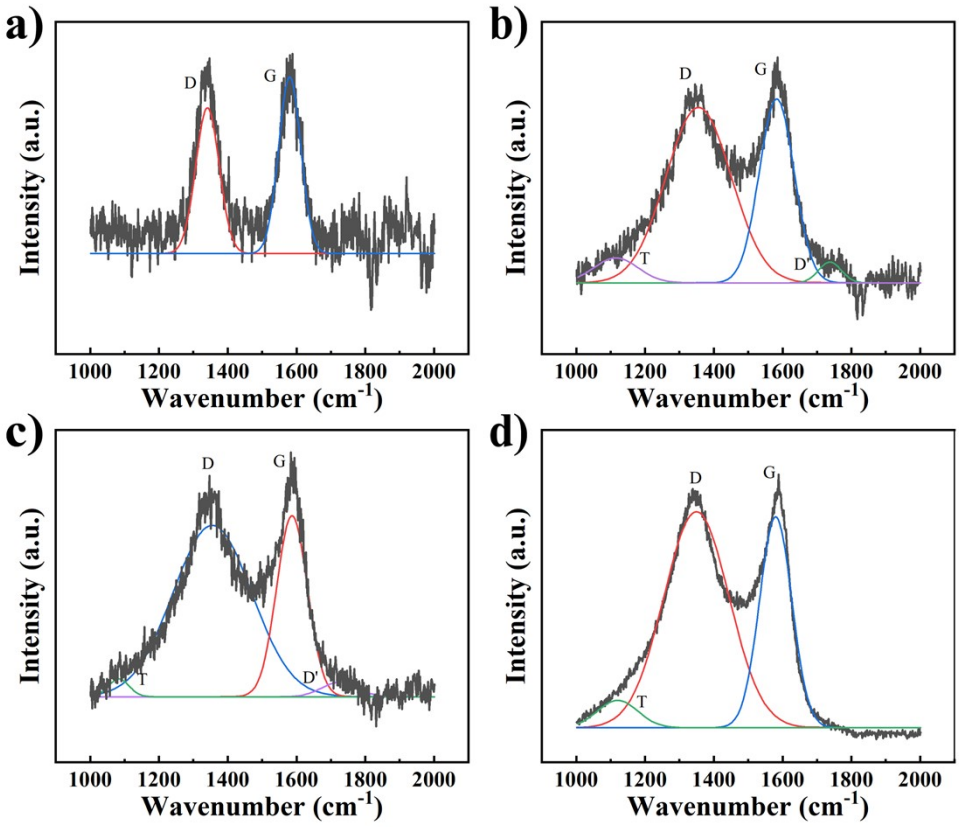

Figure S5 *Raman patterns with fitted curves for a) c-BC-1050, b) c-BP_2-1050, c) c-BP_5-1050, and d) c-BP_8-1050.*

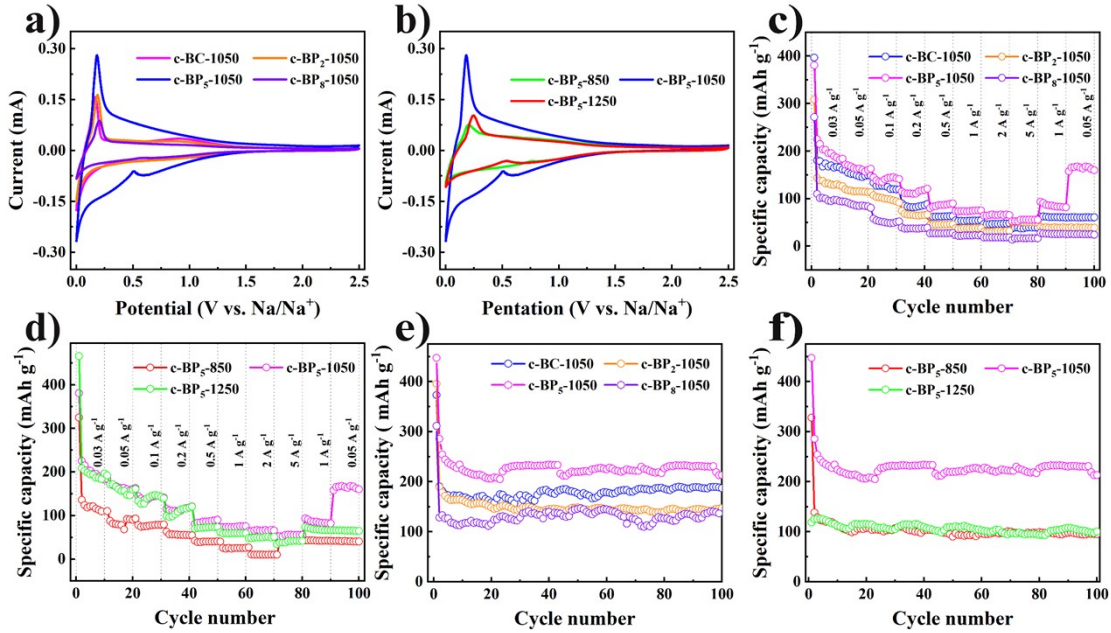

Figure S6 *The electrochemical performance of different carbon anodes: a) and b) for the CV curves at 0.1 mV s^{-1}; c) and d) for the rate performance; e) and f) for the cycle performance at 0.1 A g^{-1}.*

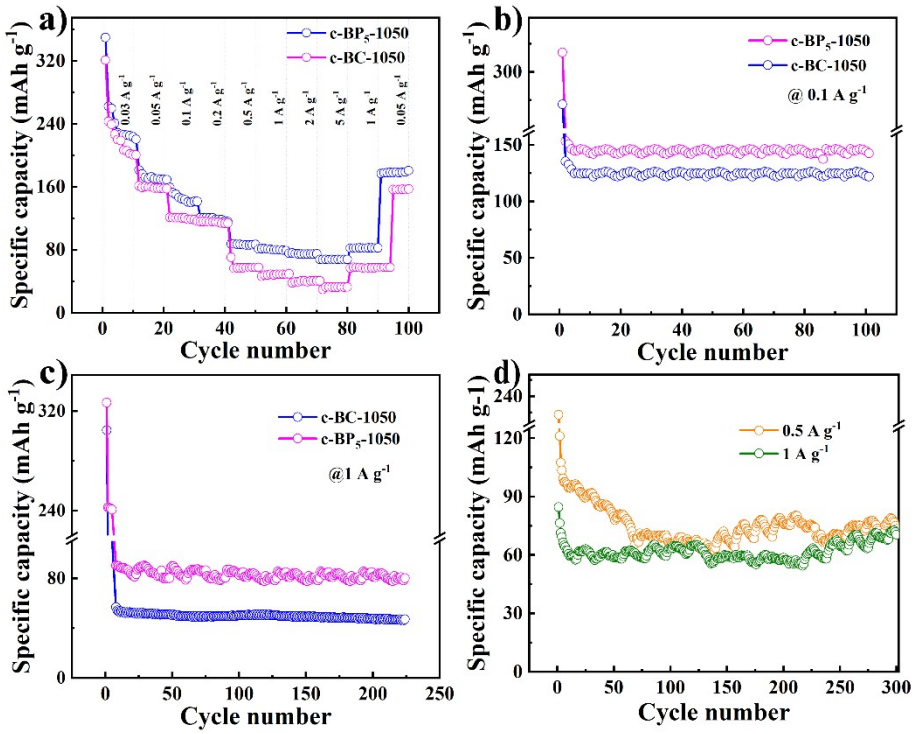

Figure S7 *The electrochemical performance of c-BP_5-1050 and c-BC-1050 with areal loading of 1.3-1.5 mg cm^{-2}: a) rate performance; b)cycle stabilty at 0.1 A g^{-1}, and c) 1 A g^{-1} ; d) the cycle performance of c-BP_5-1050 with areal loading of 0.8 mg cm^{-2} at 0.5 A g^{-1} and 1 A g^{-1} for 300 cycles.*

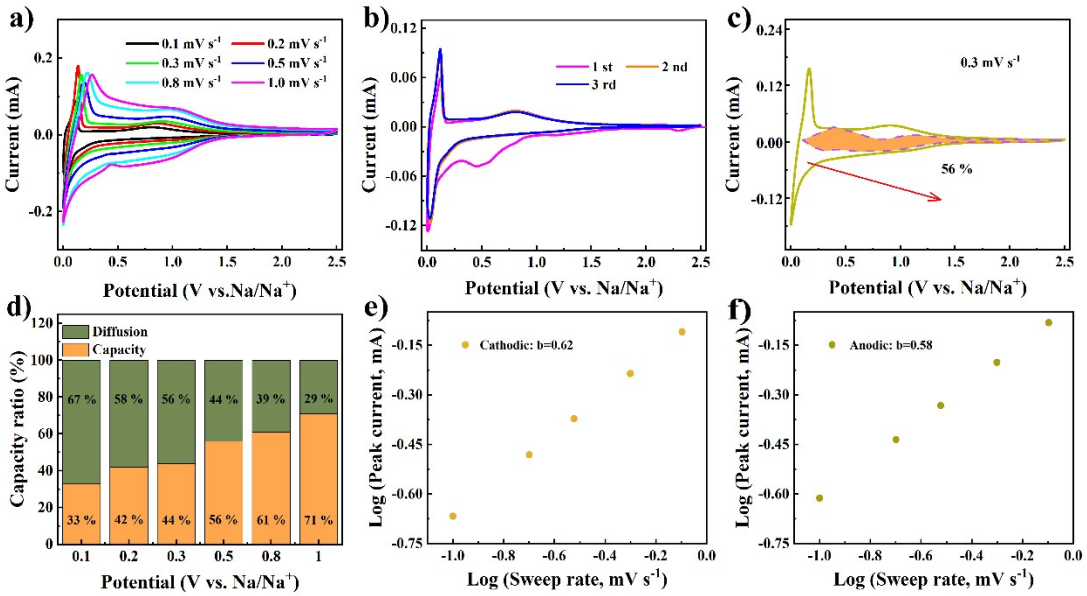

Figure S8 *a) CV curves at scan rates from 0.1 to 1.0 mV s^{-1} for c-BC-1050 carbon anode; b) CV curves of c-BC-1050 carbon anode at a scan rate of 0.1 mV s^{-1}; c) the capacitive contribution of c-BC-1050 at 0.3 mV s^{-1}; d) the capacity ratio of capacitive- and diffusion-controlled charge versus from 0.1 to 1 mV s^{-1} for c-BC-1050; and e) cathodic and f) anodic of the relationship between peak current and scan rate.*

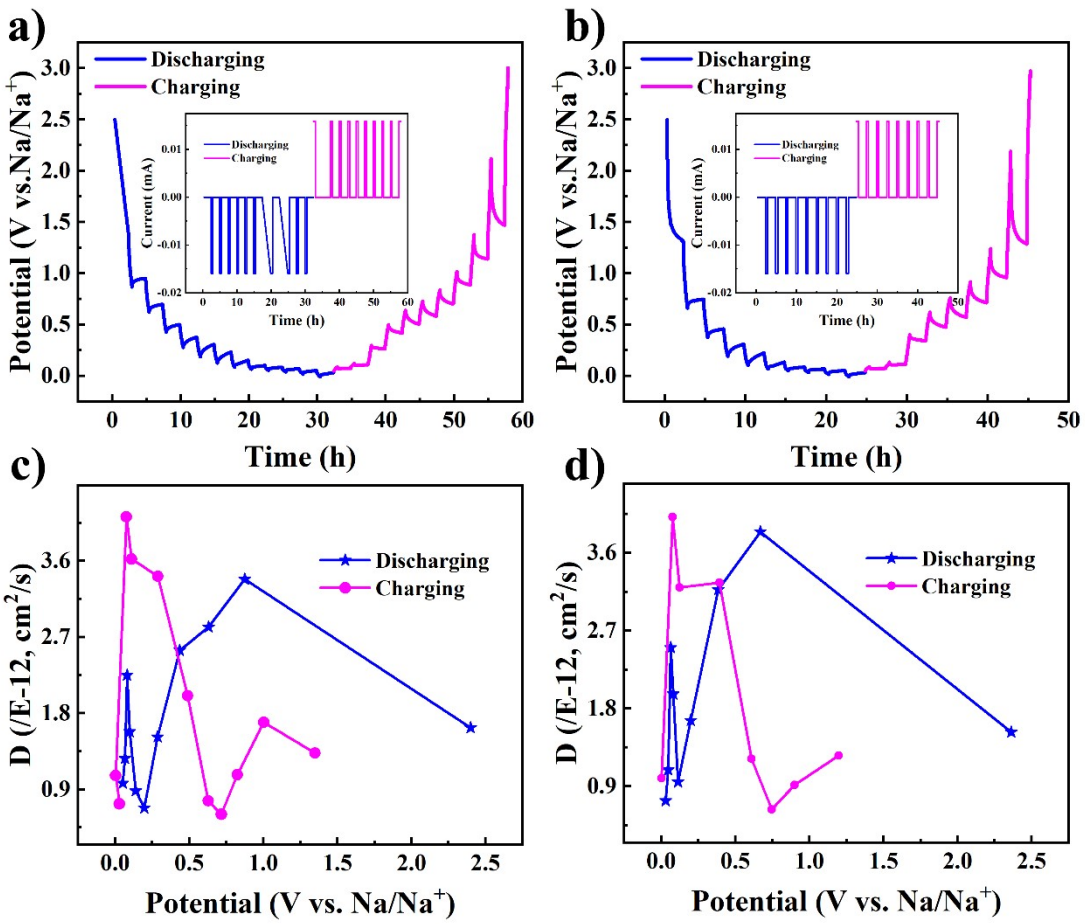

Figure S9 *GITT measurements. The potential profiles of a) c-BP_2-1050 and c) c-BP_8-1050 anodes at the discharging/charging states (inset images are the relationship of current and time); the calculating sodium-ion diffusion coefficient for b) c-BP_2-1050 and d) c-BP_8-1050 anodes at the discharging/charging states.*

Table S1 *Parameters of different carbon materials.*

Sample	Peak position(°)		d_{002}(nm)	L_c (nm)	I_D/I_G
	(*002*)	(*100*)			
c-BC-1050	25.634	42.694	0.347	0.136	1.264
c-BP_2-1050	23.558	42.749	0.377	2.000	1.784
c-BP_8-1050	26.788	42.567	0.332	0.708	2.389
c-BP_5-1050	22.964	43.113	0.387	0.622	2.069
c-BP_5-850	26.967	43.192	0.330	1.985	-
c-BP_5-1250	25.899	42.749	0.344	0.515	-

Peak positions of (*002*) and (*100*), the average interlayer spacing d_{002}, the average thickness (L_c), and the number (N) of the stacked graphene sheets in resulting carbons from XRD patterns. The d_{002} could be conducted according to Bragg's equation: d_{002} (nm) $=\lambda/2\sin\theta$, where 2θ is the diffraction angle, λ is the wavelength of the incident X-ray excitation beam (λ=0.154 nm). The L_c of the order-layered segments is estimated by the Debye-Scherrer equation. $L_c=0.89\lambda/\beta_{002}cos\theta_{002}$, in which θ_{002} and β_{002} represent the (*002*) peak position and peak width at its half height, respectively. The number N is calculated by L_c/d_{002}.

Table S2 *The physical parameters and electrochemical performance comparison of various carbon anodes recently reported using cellulose as precursors for SIB.*

Sample	S_{BET} (m^2 g^{-1})	I_D/I_G	Areal Load (mg cm^{-2})	Rate performance		Reference
				Current density (mA g^{-1})	Capacity (mAh g^{-1})	
Natural cotton	38	-	2.5-3.5	150	275	[1]
				300	180	
Bleached pulp	377	1.05	1-1.2	2000	85	[2]
TEMPO- bleached pulp	126	-	2.5	100	196	[3]
cellulose nanocrystals films	145.56	1.07	2	20	375	[4]
				200	220	
Bacterial cellulose films	128	1.90	0.5	200	271	[5]
				200	205	
Hard carbon	-	-	1.5	50	310	[6]
				5000	145	
Magnolia grandiflora Lima leaves	95.7	1.09	-	500	185.4	[7]
				2000	126.8	
Cellulose	117	1.49	2.5	200	200	[8]
c-BC-1050	58.40	1.26	0.8	30	396.6	**This work**
				2000	46.8	
			1.3-1.5	30	200.4	
				2000	37.9	
c-BP_5-1050	141.03	2.07	0.8	30	380.7	**This work**
				2000	64.1	
			1.3-1.5	30	225.6	
				2000	75.4	

References

[1] Li Y, Hu Y-S, Titirici M-M, et al. Hard Carbon Microtubes Made from Renewable Cotton as High-Performance Anode Material for Sodium-Ion Batteries[J]. Advanced Energy Materials, 2016, 6(18): 1600659.

[2] Luo W, Schardt J, Bommier C, et al. Carbon Nanofibers Derived from Cellulose Nanofibers as a Long-Life Anode Material for Rechargeable Sodium-Ion Batteries[J]. Journal of Materials Chemistry A, 2013, 1(36): 10662-10666.

[3] Shen F, Zhu H, Luo W, et al. Chemically Crushed Wood Cellulose Fiber Towards High-Performance Sodium-Ion Batteries[J]. ACS Appl Mater Interfaces, 2015, 7(41): 23291-23296.

[4] Zhu H, Shen F, Luo W, et al. Low Temperature Carbonization of Cellulose Nanocrystals for High Performance Carbon Anode of Sodium-Ion Batteries[J]. Nano Energy, 2017, 33: 37-44.

[5] Yang H, Xu R , and Yu Y. A Facile Strategy toward Sodium-Ion Batteries with Ultra-Long Cycle Life and High Initial Coulombic Efficiency: Free-Standing Porous Carbon Nanofiber Film Derived from Bacterial Cellulose[J]. Energy Storage Materials, 2019, 22: 105-112.

[6] Xia J L, Yan D, Guo L P, et al. Hard Carbon Nanosheets with Uniform Ultramicropores and Accessible Functional Groups Showing High Realistic Capacity and Superior Rate Performance for Sodium-Ion Storage[J]. Advanced Materials, 2020, 32(21): 2000447.

[7] Zhu Z, Zhong W, Zhang Y, et al. Elucidating Electrochemical Intercalation Mechanisms of Biomass-Derived Hard Carbon in Sodium-/Potassium-Ion Batteries[J]. Carbon Energy, 2021: 1-13.

[8] Qiu S, Xiao L, Sushko M L, et al. Manipulating Adsorption-Insertion Mechanisms in Nanostructured Carbon Materials for High-Efficiency Sodium Ion Storage[J]. Advanced Energy Materials, 2017, 7(17): 1700403.